

# Bioresorbable vascular scaffolds versus everolimus-eluting stents: a biomechanical analysis of the ABSORB III Imaging substudy



Arnav Kumar<sup>1</sup>, MD, MSCR; Bill D. Gogas<sup>1</sup>, MD, PhD; Elizabeth W. Thompson<sup>1</sup>, BS; Grady Murphy Burnett<sup>1</sup>, BS; David Molony<sup>1</sup>, PhD; Hossein Hosseini<sup>1</sup>, MD; Karthic Chandran<sup>1</sup>, MD; Adrien Lefieux<sup>1</sup>, PhD; Yasuhiro Honda<sup>2</sup>, MD; Joo Myung Lee<sup>1</sup>, MD, PhD; Patrick W. Serruys<sup>4</sup>, MD, PhD; Dean J. Kereiakes<sup>5</sup>, MD; Gregg W. Stone<sup>6</sup>, MD; Habib Samady<sup>1\*</sup>, MD

1. *Andreas Gruentzig Cardiovascular Center, Emory University School of Medicine, Atlanta, GA, USA*; 2. *Stanford Cardiovascular Institute, Stanford, CA, USA*; 3. *Abbott Vascular, Inc., Santa Clara, CA, USA*; 4. *Department of Cardiology, National University of Ireland, Galway, Ireland*; 5. *The Christ Hospital Heart and Vascular Center, Cincinnati, OH, USA*; 6. *Columbia University Medical Center, New York, NY, USA*

A list of study collaborators can be found in the Appendix paragraph.

GUEST EDITOR: Alec Vahanian, MD, PhD; *Department of Cardiology, Hôpital Bichat-Claude Bernard, and University Paris VII, Paris, France*

This paper also includes supplementary data published online at: <https://eurointervention.pronline.com/doi/10.4244/EIJ-D-19-01128>

## KEYWORDS

- bioresorbable scaffolds
- intravascular ultrasound
- QCA
- stent thrombosis

## Abstract

**Aims:** The Absorb bioresorbable vascular scaffold (BVS) has high rates of target lesion failure (TLF) at three years. Low wall shear stress (WSS) promotes several mechanisms related to device TLF. We investigated the impact of BVS compared to XIENCE V (XV) on coronary WSS after device deployment.

**Methods and results:** In the prospective, randomised, controlled ABSORB III Imaging study (BVS [n=77] or XV [n=36]), computational fluid dynamics were performed on fused angiographic and intravascular ultrasound (IVUS) images of post-implanted vessels. Low WSS was defined as <1 Pa. There were no differences in demographics, clinical risks, angiographic reference vessel diameter or IVUS minimal lumen diameter between BVS and XV patients. A greater proportion of vessels treated with BVS compared to XV demonstrated low WSS across the whole device (BVS: 17/77 [22%] vs XV: 2/36 [6%], p<0.029). Compared to XV, BVS demonstrated lower median circumferential WSS (1.73 vs 2.21 Pa; p=0.036), outer curvature WSS (p=0.026), and inner curvature WSS (p=0.038). Similarly, BVS had lower proximal third WSS (p=0.024), middle third WSS (p=0.047) and distal third WSS (p=0.028) when compared to XV. In a univariable logistic regression analysis, patients who received BVS were 4.8 times more likely to demonstrate low WSS across the scaffold/stent when compared to XV patients. Importantly, in a multivariable linear regression model, hypertension (beta: 0.186, p=0.023), lower contrast frame count velocity (beta: -0.411, p<0.001), lower post-stent residual plaque burden (beta: -0.338, p<0.001), lower % underexpanded frames (beta: -0.170, p=0.033) and BVS deployment (beta: 0.251, p=0.002) remained independently associated with a greater percentage of stented coronary vessel areas exposed to low WSS.

**Conclusions:** In this randomised controlled study, the Absorb BVS was 4.8 times more likely than the XV metallic stent to demonstrate low WSS. BVS implantation, lower blood velocity and lower residual post-stent plaque burden were independently associated with greater area of low WSS.

\*Corresponding author: *Interventional Cardiology, Emory University Medical Center, 1364 Clifton Road, Suite F606, Atlanta, GA 30322, USA. E-mail: [hsamady@emory.edu](mailto:hsamady@emory.edu)*

## Abbreviations

<b>BVS</b>	bioresorbable vascular scaffold
<b>CFD</b>	computational fluid dynamics
<b>IVUS</b>	intravascular ultrasound
<b>IQR</b>	interquartile range
<b>LAD</b>	left anterior descending
<b>NO</b>	nitric oxide
<b>RVD</b>	reference vessel diameter
<b>SD</b>	standard deviation
<b>UE</b>	underexpansion
<b>WSS</b>	wall shear stress
<b>XV</b>	XIENCE V
<b>3D</b>	three-dimensional

## Introduction

Bioresorbable vascular scaffolds (BVS) (Absorb™; Abbott Vascular, Santa Clara, CA, USA) were introduced as a transformative technology designed to improve the long-term outcomes of metallic stents by reducing the risk of stent thrombosis, stent fracture and neoatherosclerosis. After encouraging early data from ABSORB I and ABSORB II<sup>1</sup>, the pivotal randomised prospective ABSORB III multicentre study demonstrated non-inferiority of BVS compared to the XIENCE V® (XV) metallic stent (Abbott Vascular) with respect to one-year target lesion failure (TLF)<sup>2</sup>. However, more recent data comparing outcomes beyond one year from the ABSORB trials confirmed higher rates of target vessel failure (TVF) largely due to greater scaffold thrombosis and raised safety concerns regarding current-generation BVS, resulting in discontinuation of commercial sales by the manufacturer in September 2017<sup>3</sup>.

Nevertheless, if these safety concerns can be overcome, biodegradable scaffolds may yet prove to address issues related to long-term metallic caging including endothelial dysfunction, inflammation related to metal or durable polymer, stent fracture driving in-stent restenosis, and neoatherosclerosis. Therefore, understanding the mechanisms of scaffold failure can inform the future design of biodegradable scaffolds. Potential mechanisms of BVS failure include the presence of disturbed flow with recirculation zones related to the larger struts, ongoing inflammation and endothelial dysfunction associated with polymer degradation, late recoil and intraluminal scaffold dismantling<sup>4</sup>.

Compared to XV, BVS have been shown to cause less vascular straightening and preserved vessel curvature<sup>5</sup>. This vessel or macro level biomechanical effect of BVS may have a favourable impact on wall shear stress (WSS). Physiological WSS (1-2.5 Pa) is thought to be important in promoting a uniform neointimal response and stent healing<sup>6</sup>. However, at the strut or micro level, the larger struts of BVS (157 µm) compared with contemporary metallic stents (75-90 µm) create zones of fluid disturbance, with higher WSS on the tops of the struts and low WSS with flow separation and stagnation zones immediately proximal and distal to the struts<sup>7,8</sup>. Zones of low WSS after stent implantation have been associated with neointimal hyperplasia and subsequent TLF<sup>9</sup>.

These complex macro and micro level differences in WSS responses between BVS and XV may be accentuated by differential stent underexpansion (UE) and recoil of BVS versus XV when implanted in fibrotic or calcified coronary plaques resulting in non-uniform luminal geometry, which may affect the incidence of restenosis and possibly scaffold thrombosis<sup>6</sup>. Low WSS probably promotes neointimal hyperplasia through interactions of smooth muscle cells with shear-sensing endothelial cells as well as by promoting plaque development and a vulnerable plaque phenotype, which may be a precursor of neoatherosclerosis<sup>9</sup>.

To evaluate the impact of BVS on coronary WSS after device deployment, we investigated the differences in vascular geometry, UE and WSS distribution in patients randomised to BVS versus XV in the intravascular ultrasound (IVUS) arm of the ABSORB III Imaging substudy.

## Methods

### STUDY POPULATION AND STUDY DESIGN

The IVUS arm of the ABSORB III Imaging study (clinicaltrials.gov NCT01751906) was a prospectively designed randomised controlled trial in which 150 patients were randomised 2:1 to BVS versus XV similar to the larger clinical trial<sup>10</sup>. An independent core lab (Stanford University School of Medicine, Stanford, CA, USA) received and stored angiographic and IVUS images. These images were then transferred to another independent core lab (Emory University Medical School, Atlanta, GA, USA) for three-dimensional (3D) reconstruction and post-processing (**Supplementary Appendix 1**).

### POST-PROCESSING COMPUTATIONS

For quantitative comparisons, mean circumferential WSS across the total stented segments, along with proximal, middle and distal segments and inner and outer curvatures<sup>11</sup> of the stent were computed (**Figure 1**). Low WSS was defined as <1 Pa<sup>12,13</sup>. A patient demonstrating average WSS <1 Pa across the total stented area

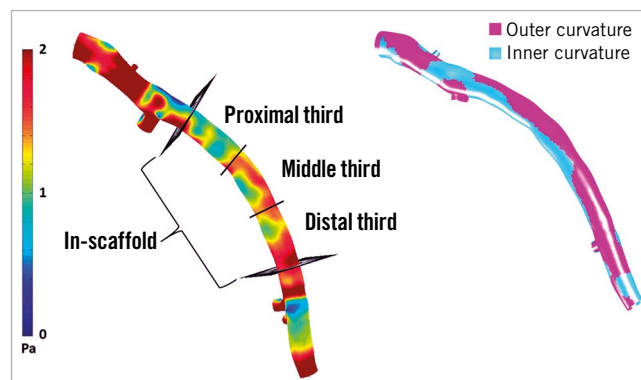


**Figure 1.** Wall shear stress (WSS) measurements after post-processing. WSS was calculated across the whole stented area, and across proximal, middle, and distal segments along with outer and inner curvatures.

of the vasculature was identified as showing low WSS across the total stent. We also identified IVUS frames with circumferential WSS <1 Pa. To identify the stented vessel length exposed to low WSS, we computed the cumulative distance between successive IVUS frames with low WSS. This length was then divided by the total length of the stented vessel and multiplied by 100 to obtain the percentage length exposed to low WSS.

### STENT UNDEREXPANSION AND ECCENTRICITY INDEX

Given that there is no well accepted definition of stent UE and the critical importance of the relationship between WSS and UE, IVUS UE was determined using three different methods – a proximal/distal reference method, a tapering reference method and the MUSIC criteria (Multicentre Ultrasound Stenting in Coronaries study) (Supplementary Figure 1)<sup>14,15</sup>.

In addition, we calculated eccentricity index (EI%) across the device (Supplementary Figure 2).

### STATISTICAL ANALYSIS

Continuous variables are summarised as mean and standard deviation (SD) or median and interquartile range (IQR), as appropriate, and categorical variables as count and proportion. Categorical data are presented as absolute numbers and percentages. Comparisons between groups were performed using the Student's t-test, Wilcoxon rank-sum test, chi-square test, and Fisher's exact test, as appropriate. The association between patients with low WSS across the total stented section and the clinical, angiographic and IVUS-derived pre- and post-stent variables was investigated using a logistic regression analysis. Since 19 patients demonstrated low WSS across the total stent, only a univariable logistic regression model was constructed. Subsequently, both univariable and multivariable linear regression models were used to investigate the relationship between clinically relevant pre- and post-stent variables and percentage of stent length exposed to low WSS. A p-value of <0.05 was considered statistically significant. Analyses were performed using SPSS, Version 24.0 (IBM Corp., Armonk, NY, USA).

## Results

### STUDY POPULATION

A total of 141 patients were enrolled in the ABSORB III Imaging study (Supplementary Figure 3). IVUS images were not available at the IVUS core laboratory in five patients. A further 22 patients did not have adequate IVUS image quality or sufficient pullback length in the stented segments of the vessels for computational fluid dynamics (CFD) and post-processing for WSS analysis. One patient had received both a BVS and an XV stent and hence was not included in the final analysis.

Supplementary Table 1 shows the baseline features of the 113 patients who were included in the final analysis. The BVS and the XV groups did not differ in terms of demographics, clinical variables, pre- and post-vessel and lesion-specific angiographic or percentage UE (Supplementary Appendix 2). The BVS patients demonstrated higher EI% when compared with XV patients ( $p=0.006$ ).

In addition, only four (3.5%) patients had a stent placed in a vessel with a reference vessel diameter (RVD) <2.5 mm. Interestingly, all four patients received a BVS scaffold.

### STENT-/VESSEL-LEVEL WALL SHEAR STRESS ANALYSIS

A significantly greater proportion of patients,  $n=17/77$  (22%), in the BVS group demonstrated low WSS across the total scaffold while only 2/36 (6%) patients in the XV stent group demonstrated low WSS,  $p=0.029$  (Figure 2). Table 1 demonstrates that median circumferential ( $p=0.036$ ), inner curvature ( $p=0.038$ ), and outer curvature ( $p=0.026$ ) WSS were lower in BVS compared to XV. To investigate further any regional haemodynamic differences across platforms, we divided the stented segments into proximal, middle

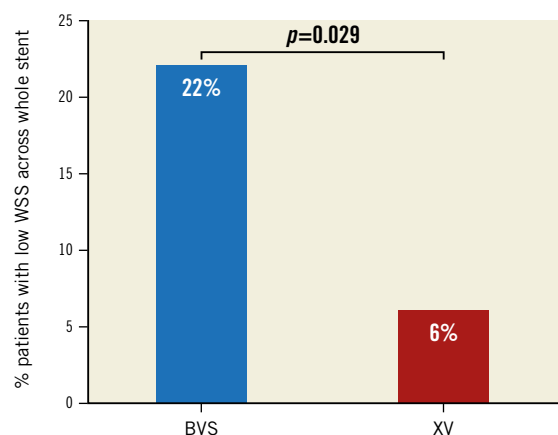


Figure 2. Percentage low WSS across stent platforms. Bar graphs represent the percentage of patients demonstrating low WSS in the BVS (17/77 [22%]) and XV (2/36 [6%]) groups,  $p=0.029$ .

Table 1. Wall shear stress calculated in various segments of BVS when compared to XV.

Stent-level analysis	BVS (n=77)	XIENCE (n=36)	p-value (non-parametric)
Total stent WSS (Pa)	1.73 (1.07, 2.59)	2.21 (1.39, 2.99)	0.036
Stent inner curvature WSS (Pa)	1.54 (1.1, 2.24)	1.91 (1.36, 2.82)	0.038
Stent outer curvature WSS (Pa)	1.61 (1.15, 2.36)	2.34 (1.4, 3.17)	0.026
Proximal stent WSS (Pa)	1.80 (0.93, 2.83)	2.31 (1.36, 3.32)	0.024
Middle stent WSS (Pa)	1.66 (0.93, 2.76)	2.21 (1.30, 2.97)	0.047
Distal stent WSS (Pa)	1.53 (0.72, 2.58)	1.92 (1.16, 2.80)	0.028
<b>Frame-level analysis</b>			
% Total stent length exposed to low WSS	24±36	7±22	0.006
% Proximal stent length exposed to low WSS	22±38	7±24	0.005
% Middle stent length exposed to LWSS	23±36	7±23	0.006
% Distal stent length exposed to LWSS	27±40	7±20	0.002
Values are median (interquartile range) or mean (±SD). BVS: Absorb bioresorbable vascular scaffold; WSS: wall shear stress; %: percentage			

and distal segments. We found that mean proximal ( $p=0.024$ ), middle ( $p=0.047$ ) and distal segment WSS ( $p=0.028$ ) was also lower in BVS compared to XV.

**Figure 3A** shows the shear stress image from a patient who received a BVS, demonstrating low WSS across the whole scaffold, including the inner and outer curvatures as well as the proximal, middle and distal segments. In contrast, **Figure 3B** displays a shear stress image from a patient who received an XV, demonstrating higher, more physiologic WSS values in the corresponding stented segments. Median WSS in the four patients with RVD  $<2.5$  mm was 1.40 (0.9, 2.58) Pa, while median WSS in 109 patients with RVD  $>2.5$  mm was 1.94 (1.28, 2.85) Pa,  $p=0.484$ .

### STENT-/VESSEL-LEVEL PREDICTORS OF LOW WALL SHEAR STRESS

Lower contrast frame count velocity (OR: 0.961,  $p<0.001$ ), lower post-stent residual plaque burden (OR: 0.917,  $p=0.018$ ), lower percentage of underexpanded frames (OR: 0.172,  $p=0.030$ ), higher EI% (OR: 1.148,  $p=0.013$ ) and use of BVS (OR: 4.817,  $p=0.043$ ) were associated with low WSS across the stent/scaffold platform (**Table 2**).

### FRAME-LEVEL WSS ANALYSIS

The BVS platform had a greater percentage of total scaffold length exposed to low WSS compared to XV ( $24\pm 36\%$  vs  $7\pm 22\%$ ,  $p<0.001$ ) (**Table 1**). Similarly, the proximal ( $p=0.005$ ), middle ( $p=0.006$ ) and distal segments ( $p=0.002$ ) of BVS demonstrated a significantly greater percentage of scaffold length with low WSS compared to XV.

**Table 2. Association between BVS and low wall shear stress using logistic regression analysis.**

Variables	OR (95% CI)	p-value
<b>Clinical characteristics</b>		
Age, per year increase	1.003 (0.960-1.048)	0.882
Male	2.659 (0.820-8.626)	0.103
Diastolic blood pressure, per unit increase (mmHg)	1.021 (0.975-1.069)	0.387
Hypertension	6.522 (0.827-51.426)	0.075
Diabetes mellitus	0.652 (0.173-2.453)	0.527
Left anterior descending PCI	2.462 (0.863-7.027)	0.092
Contrast frame count velocity, per mm/sec increase	0.961 (0.940-0.982)	$<0.001$
IVUS post-stent MLD, per mm increase	1.433 (0.393-5.228)	0.586
IVUS post-stent residual plaque burden, per % increase	0.917 (0.854-0.985)	0.018
Underexpanded frames within stent (MUSIC criteria), per % increase	0.172 (0.035-0.842)	0.030
Eccentricity index, per % increase	1.148 (1.030-1.280)	0.013
BVS	4.817 (1.049-22.119)	0.043

BVS: Absorb bioresorbable vascular scaffold; CI: confidence interval; IVUS: intravascular ultrasound; OR: odds ratio; PCI: percutaneous coronary interventions; %: percentage

### FRAME-LEVEL PREDICTORS OF LOW WALL SHEAR STRESS

In a univariable linear regression analysis, patients who received stents in the left anterior descending (LAD) artery (beta: 0.214,  $p=0.023$ ), those with lower contrast frame count velocity (beta:  $-0.411$ ,  $p<0.001$ ), those with lower post-stent residual plaque burden (beta:  $-0.308$ ,  $p=0.001$ ), those with a lower percentage of underexpanded IVUS frames (beta:  $-0.239$ ,  $p=0.011$ ),

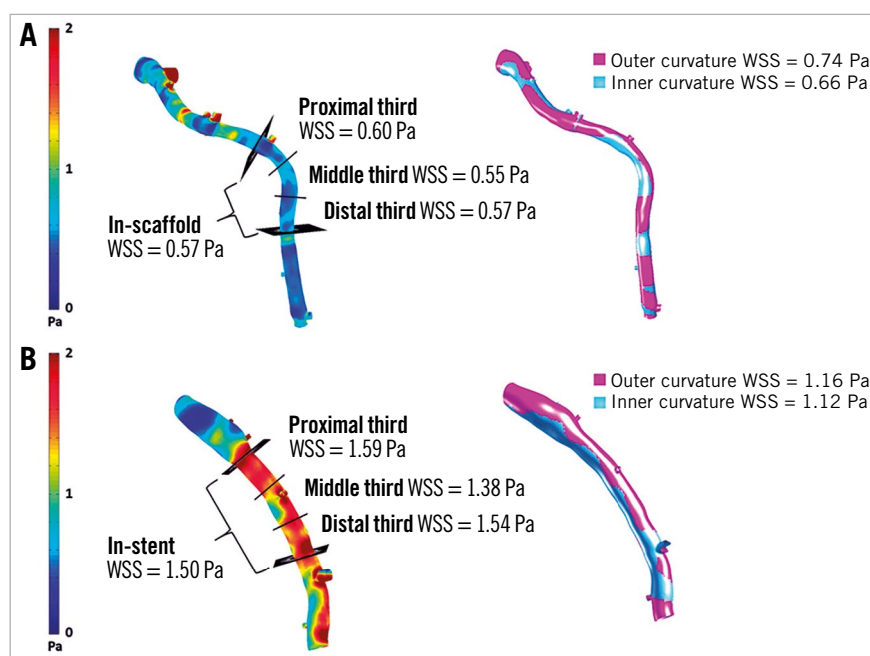


**Figure 3.** Wall shear stress (WSS) map from a patient who received a BVS demonstrating low WSS across the scaffold and proximal, middle and distal segments along with outer and inner curvatures. A) Post-processed WSS map from a patient who received an XV demonstrating higher WSS across the stent and proximal, middle and distal segments along with outer and inner curvatures (B).

those with higher EI% (beta: 0.304,  $p=0.001$ ) and those who received BVS (beta: 0.239,  $p=0.011$ ) were associated with a greater percentage of stent/scaffold area exposed to low WSS (**Table 3**). In the multivariable model, patients with a history of hypertension (beta: 0.189,  $p=0.020$ ), lower contrast frame count velocity (beta:  $-0.326$ ,  $p<0.001$ ), lower residual plaque burden after stent deployment (beta:  $-0.335$ ,  $p<0.001$ ), lower percentage of underexpanded IVUS frames (beta:  $-0.166$ ,  $p=0.035$ ) along with patients who received BVS (beta: 0.210,  $p=0.011$ ) remained independently associated with a greater percentage of stented coronary vessel areas exposed to low WSS. Higher EI% (beta: 0.145,  $p=0.081$ ) showed a trend towards demonstrating more areas of the stented vasculature exposed to low WSS.

## Discussion

The biomechanical analysis of the ABSORB III Imaging substudy demonstrates that patients randomised to BVS compared to XV had no significant differences in post-stent IVUS characteristics or UE. Importantly, patients with BVS had a significantly greater proportion of stents with low mean WSS and significantly lower WSS values across the whole stent, inner and outer curvature, as well as within the proximal, middle, and distal thirds of the stent compared with those treated with XV. Low stent WSS was associated with lower contrast velocity, less residual plaque between struts and vessel wall, less stent UE, higher eccentricity index and BVS placement. Independent predictors of greater length of low WSS were hypertension, placement of BVS, lower contrast frame count velocity, less residual plaque between struts and vessel wall, and less stent UE.

### BVS AND POST-STENT LOW WSS

Disturbed or low regional WSS within the thicker scaffolds of BVS has been associated with increased atherogenic particle residence time, increased platelet activation, regional fibrin

accumulation and promotion of prothrombotic pathways potentially resulting in scaffold thrombosis or neoatherosclerosis<sup>9,16</sup>. In addition, low WSS after stent deployment is thought to induce mechano-transduction pathways promoting inflammation and neointimal hyperplasia, resulting in stent restenosis<sup>17</sup>. At the strut level, the thicker protruding struts of the implanted BVS scaffold (157  $\mu\text{m}$ ) create a rough luminal surface and recirculation zones, resulting in low WSS predisposing patients to greater risk of scaffold thrombosis and restenosis<sup>9</sup>. Low WSS has also been associated with endothelial dysfunction and plaque propagation in patients with non-obstructive coronary artery disease (CAD)<sup>12,13</sup>. A previous observational study of patients with obstructive lesions treated with BVS (N=12) found that lower WSS was associated with neointimal hyperplasia<sup>9</sup>. In the present randomised comparison of BVS versus XV from the ABSORB III Imaging substudy, we demonstrate that BVS is independently associated with greater areas of low WSS. Other predictors of low WSS included lower blood flow velocity, history of hypertension, less UE and higher eccentricity index. The lower blood velocity and history of hypertension could reflect increased microvascular resistance, which has been related to low WSS. The triad of abnormal endothelial function, increased microvascular resistance and low WSS probably induces mechanobiological pathways that promote neointimal hyperplasia and possibly neoatherosclerosis. Interestingly, BVS demonstrated higher EI% compared to the metallic XV. Nevertheless, the results of multivariable analysis imply that BVS itself would be an important determinant for low WSS distribution even after adjusting for higher EI% (**Supplementary Appendix 3**).

Although the zones proximal and distal to struts are predisposed to having low WSS, the top of BVS struts probably display physiologic or high WSS. High WSS, through activation of platelets or matrix metalloproteinases, has been shown to predict myocardial infarction in patients with haemodynamically significant lesions<sup>18</sup>. It is important to note that the current analysis was

**Table 3. Association between BVS and % stented length demonstrating low wall shear stress using linear regression analysis.**

Variables	Univariable		Multivariable	
	Beta (95% CI)	p-value	Beta (95% CI)	p-value
Age, per year increase	-0.034 (-0.007-0.005)	0.723	0.125 (-0.001-0.009)	0.140
Males	0.127 (-0.00-0.255)	0.052	0.055 (-0.074-0.149)	0.507
Diastolic blood pressure, per unit increase (mmHg)	0.115 (-0.002-0.010)	0.227	0.016 (-0.005-0.006)	0.850
Hypertension	0.167 (-0.015-0.278)	0.077	0.189 (0.021-0.236)	0.020
Diabetes mellitus	0.128 (-0.214-0.040)	0.177	-0.086 (-0.167-0.050)	0.287
Left anterior descending PCI	0.214 (0.020-0.265)	0.023	0.130 (-0.020-0.193)	0.110
Contrast frame count velocity, per mm/sec increase	-0.411 (-0.006--0.002)	<0.001	-0.326 (-0.005--0.002)	<0.001
IVUS post-stent MLD, per mm increase	0.032 (-0.136-0.192)	0.735	0.071 (-0.077-0.202)	0.379
IVUS post-stent residual plaque burden, per % increase	-0.308 (-0.020--0.005)	0.001	-0.335 (-0.020--0.007)	<0.001
Stent IVUS frames with underexpansion (MUSIC criteria), per % increase	-0.239 (-0.375--0.050)	0.011	-0.166 (-0.286--0.10)	0.035
Eccentricity index %	0.304 (0.010-0.037)	0.001	0.145 (-0.138-2.356)	0.081
BVS	0.239 (0.040-0.301)	0.011	0.210 (0.035-0.265)	0.011

BVS: Absorb bioresorbable vascular scaffold; CI: confidence interval; IVUS: intravascular ultrasound; OR: odds ratio; PCI: percutaneous coronary interventions; %: percentage

performed on reconstructed angiographic and IVUS images that may not have the spatial resolution to investigate strut-level heterogeneity in WSS. In addition, after stent placement, the vessel lumen usually does not have enough residual stenosis to result in flow acceleration sufficient to cause extremely high WSS values. Furthermore, we did not find any differences in UE that might drive WSS heterogeneity between the two stent platforms.

### IMPACT OF UNDEREXPANSION ON WSS

It has been argued that the BVS platform, due to its markedly lower tensile strength, lower tensile modulus of elasticity and thicker and wider struts, has different expansion characteristics compared to metallic stents, particularly when deployed in the clinical setting of complex coronary atherosclerosis<sup>19</sup>. Greater attention to lesion preparation, including more aggressive balloon sizing and higher pressure inflations for predilatation and plaque modification prior to scaffold deployment, has been advocated<sup>20</sup>. Without such meticulous attention to detail, it was expected that patients receiving BVS would have more scaffold UE compared to those receiving metallic XV stents, exposing them to the well documented adverse consequences of stent UE.

Somewhat surprisingly in the present study, we found similar rates of UE in both stent platforms using three different methodologies to identify stent or scaffold UE. Hence, device UE is unlikely to have contributed to a greater prevalence of low WSS areas in BVS compared to XV. From a fluid dynamics standpoint, stenosis created by an underexpanded stent would result in lower WSS proximal and distal to the underexpanded segment and higher WSS within the underexpanded segment. Indeed, we demonstrate that lower rather than higher rates of stent UE were associated with low WSS. The corollary to this observation is that, regardless of stent type, underexpanded segments demonstrated higher WSS. These data illustrate the complex relationship between stent UE and WSS and suggest that further investigation is warranted.

### RELATIONSHIP BETWEEN STENT PLATFORM, VESSEL SIZE AND WALL SHEAR STRESS

Previous studies have indicated a higher prevalence of scaffold thrombosis when a BVS was implanted in a smaller vessel (<2.5 mm by quantitative coronary angiography [QCA]) and in patients with higher residual minimum lumen diameter (MLD)<sup>21</sup>. However, in our study, the median RVDs were similar in patients who received BVS and XV. Median WSS was also numerically but not statistically lower in patients with an RVD <2.5 mm and therefore vessel size by itself could not explain the observed lower WSS in the BVS group. Interestingly, there was a trend towards a greater post-stent MLD in the XV group, which could have explained slightly higher WSS in the XV group. However, frame-level analysis demonstrated that BVS were associated with a greater percentage of low WSS lengths even after adjusting for various clinical, angiographic and IVUS-related predictors of low WSS including residual MLD.

### THE HAEMODYNAMIC PROFILE OF BVS: WHAT DOES THE FUTURE HOLD?

Taken together, our findings suggest that the association between BVS and low WSS is probably not related to UE or differences in vessel characteristics but rather related to aspects of BVS design such as thicker strut size. The thick, rectangular BVS struts with square edges create low WSS zones while thin, circular struts with smoother edges have minimal impact on flow patterns<sup>16</sup>. Furthermore, thicker struts with higher flow disruption cause larger stagnation zones and low and oscillatory WSS areas which have been associated with greater fibrin deposition, inadequate re-endothelialisation and impaired nitric oxide (NO) production and transport, impacting on regional endothelial homeostasis that makes the strut surface more pro-thrombotic<sup>22</sup>. In addition, strut connectors that are arranged perpendicular to the flow create low WSS zones and increase the proportion of in-scaffold areas exposed to low WSS<sup>23</sup>. Hence, the non-streamlined BVS design used in the ABSORB III trial seems to predispose the post-stented vessel to low WSS which could mediate adverse healing conditions and a possible increased risk of scaffold thrombosis<sup>22</sup>. While very careful device sizing, better deployment techniques and optimisation can mitigate some of the adverse design features of the first-generation BVS, appropriate design iterations of future BVS, and other biodegradable scaffold platforms, could improve post-deployment haemodynamic profiles and perhaps outcomes.

### Limitations

Although this study represents a detailed biomechanical analysis of the largest prospectively collected, randomised controlled study of BVS versus XV, a few limitations have to be acknowledged. First, the BVS has been withdrawn from the market based on clinical outcome data. Nevertheless, there has been a continued effort to develop newer-generation BVS with thinner struts and a different design of the cross-section of the struts. In this regard, understanding biomechanical differences between BVS and metallic stents would be helpful in order to design new types of BVS in the future. Second, this is a cross-sectional biomechanical investigation of the two devices; the three-year follow-up data of the ABSORB III Imaging study are still pending. Nevertheless, having immediate post-implantation phase data about WSS between BVS and metallic stents would be important in order to interpret any changes or differences in three-year follow-up analysis. When available, the follow-up imaging data may further inform about the impact of post-stent haemodynamics on regional stent healing and failure rates. Furthermore, optical coherence tomography (OCT) has superior spatial resolution to investigate strut-level differences in WSS between different stent platforms<sup>7,9</sup>; however, the IVUS arm of the ABSORB III Imaging substudy (N=141, presented in the current manuscript) is much larger than the OCT arm (designed to be N=50). Nevertheless, OCT-based analysis may provide complementary data to the current IVUS-based analysis.

## Conclusions

In a prospective, randomised controlled study, the Absorb BVS was 4.8 times more likely than the XV metallic stent to demonstrate low WSS. BVS implantation, lower blood velocity, lower residual post-stent plaque burden and lower underexpansion rates were independently associated with greater areas of low WSS.

### Impact on daily practice

The Absorb BVS is associated with higher rates of target lesion failure and device thrombosis at three years. Low WSS may play an important role in promoting neointimal hyperplasia by promoting plaque development and possible device thrombosis. The results of this study show that BVS was 4.8 times more likely to demonstrate low WSS compared to the XV metallic stent. BVS implantation was also associated with greater areas of low WSS.

## Appendix. Study collaborators

Mohamad Raad, MD; Sonu Gupta, MD; David G. Sternheim, MD; Spencer B. King III, MD; *Andreas Gruentzig Cardiovascular Center, Emory University School of Medicine, Atlanta, GA, USA.* Kozo Okada, MD; *Division of Cardiovascular Medicine, Stanford Cardiovascular Institute, Stanford University School of Medicine, Stanford, CA, USA.* Richard J. Rapoza, PhD; Charles A. Simonton, MD; *Abbott Vascular, Inc., Santa Clara, CA, USA.* Don P. Giddens, PhD; *Wallace H. Coulter Department of Biomedical Engineering, Georgia Institute of Technology and Emory University, Atlanta, GA, USA.* Alessandro Veneziani, PhD; *Department of Mathematics and Computer Science, Emory University, Atlanta, GA, USA.* Stephen G. Ellis, MD; *Department of Cardiovascular Medicine, Heart and Vascular Institute, Cleveland Clinic, Cleveland, OH, USA.*

## Guest Editor

This paper was guest edited by Alec Vahanian, MD, PhD; *Department of Cardiology, Hôpital Bichat-Claude Bernard, and University Paris VII, Paris, France.*

## Funding

This research was funded by Abbott Vascular.

## Conflict of interest statement

P. Serruys has received personal fees from Biosensors, Micel Technologies, Sino Medical Sciences Technology, Philips/Volcano, Xeltis, and HeartFlow. D. Kereiakes is a consultant for and is on the Scientific Advisory Board of Boston Scientific, Inc., and receives research grants from Edwards Lifesciences. G. Stone is a consultant for Abbott Vascular, Volcano, and Infraredx. H. Samady has received research grants from Abbott Vascular, Medtronic, National Institutes of Health, St. Jude Medical, and Gilead. S. Ellis reports consulting fees/honoraria from Abbott Vascular, Medtronic, and Boston Scientific, and research grants from Abbott Vascular. D. Giddens is a Covanos stock owner. C. Simonton is employed by Abbott Vascular. A. Veneziani is

a Covanos stock owner. The other authors/study collaborators have no conflicts of interest to declare. The Guest Editor is a consultant for Edwards Lifesciences.

## References

- Serruys PW, Chevalier B, Dudek D, Cequier A, Carrié D, Iniguez A, Dominici M, van der Schaaf RJ, Haude M, Wasungu L, Veldhof S, Peng L, Staehr P, Grundeken MJ, Ishibashi Y, Garcia-Garcia HM, Onuma Y. A bioresorbable everolimus-eluting scaffold versus a metallic everolimus-eluting stent for ischaemic heart disease caused by de-novo native coronary artery lesions (ABSORB II): an interim 1-year analysis of clinical and procedural secondary outcomes from a randomised controlled trial. *Lancet*. 2015;385:43-54.
- Ellis SG, Kereiakes DJ, Metzger DC, Caputo RP, Rizik DG, Teirstein PS, Litt MR, Kini A, Kabour A, Marx SO, Popma JJ, McGreevy R, Zhang Z, Simonton C, Stone GW; ABSORB III Investigators. Everolimus-Eluting Bioresorbable Scaffolds for Coronary Artery Disease. *N Engl J Med*. 2015;373:1905-15.
- Ali ZA, Serruys PW, Kimura T, Gao R, Ellis SG, Kereiakes DJ, Onuma Y, Simonton C, Zhang Z, Stone GW. 2-year outcomes with the Absorb bioresorbable scaffold for treatment of coronary artery disease: a systematic review and meta-analysis of seven randomised trials with an individual patient data sub-study. *Lancet*. 2017;390:760-72.
- Yamaji K, Ueki Y, Souteyrand G, Daemen J, Wiebe J, Nef H, Adriaenssens T, Loh JP, Lattuca B, Wykrzykowska JJ, Gomez-Lara J, Timmers L, Motreff P, Hoppmann P, Abdel-Wahab M, Byrne RA, Meincke F, Boeder N, Honton B, O'Sullivan CJ, Ielasi A, Delarche N, Christ G, Lee JKT, Lee M, Amabile N, Karagiannis A, Windecker S, Räber L. Mechanisms of Very Late Bioresorbable Scaffold Thrombosis: The INVEST Registry. *J Am Coll Cardiol*. 2017;70:2330-44.
- Gomez-Lara J, Brugaletta S, Farooq V, van Geuns RJ, De Bruyne B, Windecker S, McClean D, Thuesen L, Dudek D, Koolen J, Whitbourn R, Smits PC, Chevalier B, Morel MA, Dorange C, Veldhof S, Rapoza R, Garcia-Garcia HM, Ormiston JA, Serruys PW. Angiographic geometric changes of the lumen arterial wall after bioresorbable vascular scaffolds and metallic platform stents at 1-year follow-up. *JACC Cardiovasc Interv*. 2011;4:789-99.
- McDaniel MC, Samady H. The sheer stress of straightening the curves: biomechanics of bioabsorbable stents. *JACC Cardiovasc Interv*. 2011;4:800-2.
- Gogas BD, Yang B, Piccinelli M, Giddens DP, King SB 3rd, Kereiakes DJ, Ellis SG, Stone GW, Veneziani A, Samady H. Novel 3-Dimensional Vessel and Scaffold Reconstruction Methodology for the Assessment of Strut-Level Wall Shear Stress After Deployment of Bioresorbable Vascular Scaffolds From the ABSORB III Imaging Substudy. *JACC Cardiovasc Interv*. 2016;9:501-3.
- Tenekecioglu E, Torii R, Bourantas C, Sotomi Y, Cavalcante R, Zeng Y, Collet C, Crake T, Suwannasom P, Onuma Y, Serruys PW. Difference in haemodynamic microenvironment in vessels scaffolded with Absorb BVS and Mirage BRMS: insights from a preclinical endothelial shear stress study. *EuroIntervention*. 2017;13:1327-35.
- Bourantas CV, Papafaklis MI, Kotsia A, Farooq V, Muramatsu T, Gomez-Lara J, Zhang YJ, Iqbal J, Kalatzis FG, Naka KK, Fotiadis DI, Dorange C, Wang J, Rapoza R, Garcia-Garcia HM, Onuma Y, Michalis LK, Serruys PW. Effect of the endothelial shear stress patterns on neointimal proliferation following drug-eluting bioresorbable vascular scaffold implantation: an optical coherence tomography study. *JACC Cardiovasc Interv*. 2014;7:315-24.
- Kereiakes DJ, Ellis SG, Popma JJ, Fitzgerald PJ, Samady H, Jones-McMeans J, Zhang Z, Cheong WF, Su X, Ben-Yehuda O, Stone GW. Evaluation of a fully bioresorbable vascular scaffold in patients with coronary artery disease: design of and rationale for the ABSORB III randomized trial. *Am Heart J*. 2015;170:641-51.

11. Wahle A, Lopez JJ, Olszewski ME, Vigmostad SC, Chandran KB, Rossen JD, Sonka M. Plaque development, vessel curvature, and wall shear stress in coronary arteries assessed by X-ray angiography and intravascular ultrasound. *Med Image Anal.* 2006;10:615-31.
12. Samady H, Eshtehardi P, McDaniel MC, Suo J, Dhawan SS, Maynard C, Timmins LH, Quyyumi AA, Giddens DP. Coronary artery wall shear stress is associated with progression and transformation of atherosclerotic plaque and arterial remodeling in patients with coronary artery disease. *Circulation.* 2011;124:779-88.
13. Kumar A, Hung OY, Piccinelli M, Eshtehardi P, Corban MT, Sternheim D, Yang B, Lefieux A, Molony DS, Thompson EW, Zeng W, Bouchi Y, Gupta S, Hosseini H, Raad M, Ko YA, Liu C, McDaniel MC, Gogas BD, Douglas JS, Quyyumi AA, Giddens DP, Veneziani A, Samady H. Low Coronary Wall Shear Stress Is Associated With Severe Endothelial Dysfunction in Patients With Nonobstructive Coronary Artery Disease. *JACC Cardiovasc Interv.* 2018;11:2072-80.
14. McDaniel MC, Eshtehardi P, Sawaya FJ, Douglas JS Jr, Samady H. Contemporary clinical applications of coronary intravascular ultrasound. *JACC Cardiovasc Interv.* 2011;4:1155-67.
15. Nakamura D, Wijns W, Price MJ, Jones MR, Barbato E, Akasaka T, Lee SW, Patel SM, Nishino S, Wang W, Gopinath A, Attizzani GF, Holmes D, Bezerra HG. New Volumetric Analysis Method for Stent Expansion and its Correlation With Final Fractional Flow Reserve and Clinical Outcome: An ILUMIEN I Substudy. *JACC Cardiovasc Interv.* 2018;11:1467-78.
16. Jimenez JM, Davies PF. Hemodynamically driven stent strut design. *Ann Biomed Eng.* 2009;37:1483-94.
17. Wentzel JJ, Krams R, Schuurbiens JC, Oomen JA, Kloet J, van Der Giessen WJ, Serruys PW, Slager CJ. Relationship between neointimal thickness and shear stress after Wallstent implantation in human coronary arteries. *Circulation.* 2001;103:1740-5.
18. Kumar A, Thompson EW, Lefieux A, Molony DS, Davis EL, Chand N, Fournier S, Lee HS, Suh J, Sato K, Ko YA, Molloy D, Chandran K, Hosseini H, Gupta S, Milkas A, Gogas B, Chang HJ, Min JK, Fearon WF, Veneziani A, Giddens DP, King SB 3rd, De Bruyne B, Samady H. High Coronary Shear Stress in Patients With Coronary Artery Disease Predicts Myocardial Infarction. *J Am Coll Cardiol.* 2018;72:1926-35.
19. Gogas B, Samady H. Special Stents: Bioresorbable Coronary Scaffolds. In: Samady H, Fearon W, Yeung A, King S, (eds). *Interventional Cardiology.* New York: McGraw-Hill Education; 2018. pp 495-511.
20. Stone GW, Gao R, Kimura T, Simonton C, Serruys PW. Optimum technique to reduce risk of stent thrombosis – Authors' reply. *Lancet.* 2016;388:127-8.
21. Puricel S, Cuculi F, Weissner M, Schmermund A, Jamshidi P, Nyffenegger T, Binder H, Eggebrecht H, Munzel T, Cook S, Gori T. Bioresorbable Coronary Scaffold Thrombosis: Multicenter Comprehensive Analysis of Clinical Presentation, Mechanisms, and Predictors. *J Am Coll Cardiol.* 2016;67:921-31.
22. Tenekecioglu E, Torii R, Bourantas C, Abdelghani M, Cavalcante R, Sotomi Y, Crake T, Su S, Santoso T, Onuma Y, Serruys PW. Assessment of the hemodynamic characteristics of Absorb BVS in a porcine coronary artery model. *Int J Cardiol.* 2017;227:467-73.
23. Pant S, Bressloff NW, Forrester AI, Curzen N. The influence of strut-connectors in stented vessels: a comparison of pulsatile flow through five coronary stents. *Ann Biomed Eng.* 2010;38:1893-907.

## Supplementary data

**Supplementary Appendix 1.** Methods.

**Supplementary Appendix 2.** Results.

**Supplementary Appendix 3.** Discussion.

**Supplementary Figure 1.** Derivation of underexpanded frames.

**Supplementary Figure 2.** Derivation of eccentricity index.

**Supplementary Figure 3.** Flow diagram of the study cohort.

**Supplementary Table 1.** Comparison of baseline demographics, clinical features and lesion characteristics in BVS versus XV groups.

The supplementary data are published online at:  
<https://eurointervention.pcronline.com/doi/10.4244/EIJ-D-19-01128>



## **Supplementary data**

### **Supplementary Appendix 1. Methods**

#### **Study population and study design**

The intravascular ultrasound (IVUS) arm of the ABSORB III Imaging study (clinicaltrials.gov NCT01751906) was a prospectively designed randomised controlled trial in which 150 patients were randomised 2:1 to BVS versus XV similar to the larger clinical trial. The RESTORATION (Evaluation and Comparison of three-dimensional wall shear stress patterns and neointimal healing following Percutaneous Coronary Intervention with Absorb Everolimus-Eluting Bioresorbable Vascular Scaffold Compared to XIENCE V Metallic Stent) study was a pre-specified clinical, angiographic, IVUS and computational analysis of the imaging data from the ABSORB III Imaging substudy designed to evaluate the potential differences in regional and stent-level wall shear stress (WSS) between BVS and XV [10] (**Supplementary Figure 1**).

#### **Intravascular imaging**

IVUS was performed at baseline to assess plaque burden prior to and after stent deployment as well as to evaluate stent expansion and stent apposition. Briefly, after patients had received 200 mg of intracoronary nitroglycerine, IVUS analysis was performed with a motorised pullback at 0.5 mm/sec [10].

#### **Angiographic and IVUS reconstruction of target vessels**

Angiographic and IVUS reconstructions, computational fluid dynamics (CFD) and WSS calculations were performed in the Emory University Cardiovascular Imaging Biomechanical Core Laboratory in Atlanta, GA, USA, by independent analysts who were blinded to patient clinical data.

Three-dimensional (3D) reconstructions of patient target vessels were performed through the combination of angiographic and IVUS images. The methodology for angiographic reconstruction of a patient's target vessel has been described previously [18]. Briefly, target vessels were reconstructed in QAngio XA 3D RE (Medis Medical Imaging Systems, Leiden, the Netherlands), resulting in centrelines for the target vessel. End-diastolic frames were extracted from IVUS pullbacks and the internal and external elastic lamina were manually contoured (echoPlaque 4.0; INDEC Medical Systems, Santa Clara, CA, USA) [13]. All files were exported to a MATLAB (MATLAB R2013b; MathWorks, Inc., Natick, MA, USA)

program where the IVUS contours were placed on the angiographically derived centreline and orientated according to the sequential triangulation algorithm. Side branches were added to the model as cylindrical extensions perpendicular to the vessel centreline and a final point-cloud representation of the vessel was generated. The 3D point-cloud was wrapped to create a 3D surface in Geomagic Studio 12 (Geomagic, Inc., Research Triangle Park, NC, USA). ICEM CFD (ANSYS ICEM, ANSYS 17; Ansys, Inc., Canonsburg, PA, USA), was used to add inlet and outlet extensions to ensure smooth flow transitions at the boundaries. Finally, the reconstructed geometry was meshed with tetrahedral elements and prismatic elements at the boundary layer.

### **Boundary conditions and computational fluid dynamics**

Patient-specific velocities were calculated from angiograms using the 3D contrast velocity method [18]. The boundary conditions and base assumptions used to compute WSS have been described previously [18]. Computational fluid dynamics were performed on the reconstructions using ANSYS Fluent. Fluid velocity was calculated using the contrast frame count velocity method [18]. The blood was assumed to be an incompressible Newtonian fluid with a density of  $1,050 \text{ kg/m}^3$  and a viscosity of  $0.0035 \text{ kg/m-s}$ ; the no-slip boundary condition (null velocity) was applied at the vessel wall. After computation, WSS values were exported to MATLAB and were averaged circumferentially at each IVUS frame.

### **Haemodynamic analysis**

In each IVUS pullback, the most distal and most proximal frames in the stented segment of the coronary vasculature were identified. The stented section of the vasculature was then divided into equal thirds: proximal, middle and distal segments. To distinguish between locations of “inner” versus “outer” curvature, a vector normal to the centreline was determined at each IVUS frame on the 3D reconstruction. The dot product of the normal vector with a vector from the centreline to each circumferential point on the IVUS frame was calculated. Based on this value, each circumferential point on the IVUS frame was assigned as inner if this value was greater than 0 or outer if this value was less than zero [11]. For quantitative comparisons, mean circumferential WSS across the total stented segments, along with proximal, middle and distal segments and inner and outer curvatures of the stent, were computed (**Figure 1**).

### **Detailed stent underexpansion methodologies**

In the proximal/distal reference method, upstream and downstream reference lumen areas were created by averaging frame-level cross-sectional lumen areas across segments 5 mm upstream and 5 mm

downstream to the stented region, respectively (**Supplementary Figure 2A**) [15]. The lumen areas of each frame in the proximal half of the stent were compared to the upstream reference lumen area; likewise, the lumen areas of frames in the distal half of the stented region were compared to the downstream reference lumen area. The tapering reference method for UE derives a proximal-to-distal constant tapering of the vessel cross-sectional lumen area using the same 5 mm upstream and 5 mm downstream reference segments (**Supplementary Figure 2B**). In the MUSIC criteria, the reference lumen area is computed by averaging the mean cross-sectional lumen areas in the upstream and downstream segments. The cross-sectional lumen area of each frame in the stented segment was then compared to the reference lumen areas by each method. A lumen area of <90% compared to the reference lumen area was defined as being an underexpanded frame. For the MUSIC criteria, if a stented segment frame lumen area was <100% of the minimum lumen area (MLA of upstream/downstream segment), that frame was also identified as an underexpanded frame [14].

### **Lumen eccentricity**

Frame-by-frame lumen eccentricity was calculated as (major diameter - minor diameter)/major diameter (**Supplementary Figure 2**). For each segment of interest (stented portion of the coronary vasculature), we calculated a mean eccentricity index. These values were then multiplied by 100 to derive EI%. A value of 0 indicates a completely circular lumen while larger values indicate increased eccentricity.

## **Supplementary Appendix 2. Results**

**Supplementary Table 1** demonstrates the baseline features of the 113 patients who were included in the final analysis. In addition, we had information regarding predilatation in 59 BVS patients and 22 XV patients. The mean number of predilatation balloons used in BVS ( $1.73 \pm 1.31$ ) was similar to the mean number of post-dilatation balloons used in patients who received XV ( $1.73 \pm 1.08$ ) ( $p=0.996$ ). Maximum balloon pressure used during predilatation was also similar, BVS ( $12.50 \pm 3.60$  atm) and XV ( $12.59 \pm 4.26$  atm) ( $p=0.924$ ).

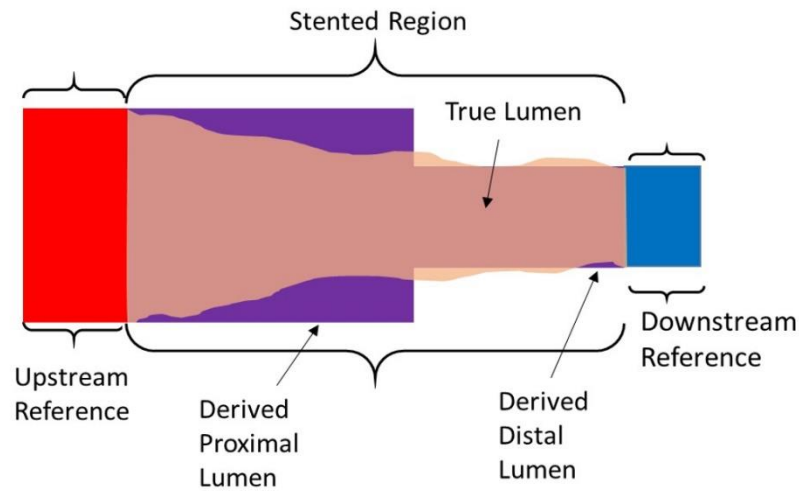
In terms of post-dilatation, mean post-dilatation balloon diameter in BVS was  $3.26 \pm 0.46$  mm which was similar to the mean post-dilatation balloon diameter in XV ( $3.24 \pm 0.38$  mm,  $p=0.845$ ). The maximum post-dilatation balloon pressure in the BVS group was  $15.11 \pm 3.63$  atm which was again similar to the XV group ( $16.46 \pm 2.88$  atm,  $p=0.186$ ).

### **Supplementary Appendix 3. Discussion**

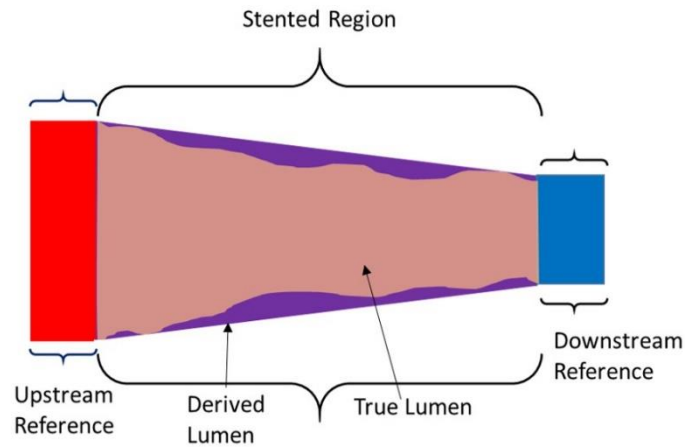
Interestingly, patients who received a LAD stent/scaffold demonstrated a trend towards low WSS across their stents (**Table 2**). While this association was not statistically significant, differences of shear stress distribution between LAD and non-LAD vessels might be related to variations in disturbed flow due to differences in size, number and location of major bifurcations as well as location of major curvatures [6].

BVS showed higher EI% compared to XV. There might be several potential explanations for higher eccentricity index in BVS. First, lower radial strength in BVS would have a higher chance of eccentric stent expansion according to plaque distribution. Second, higher post-implantation angulation in BVS would be another possible explanation for higher EI% in BVS. Third, weaker strut strength of BVS might have resulted in an uneven distribution of stent struts after expansion. Nevertheless, the results of multivariable analysis imply that the BVS itself would be an important determinant for low WSS distribution, even after adjusting for the confounding effect of EI%.

A.

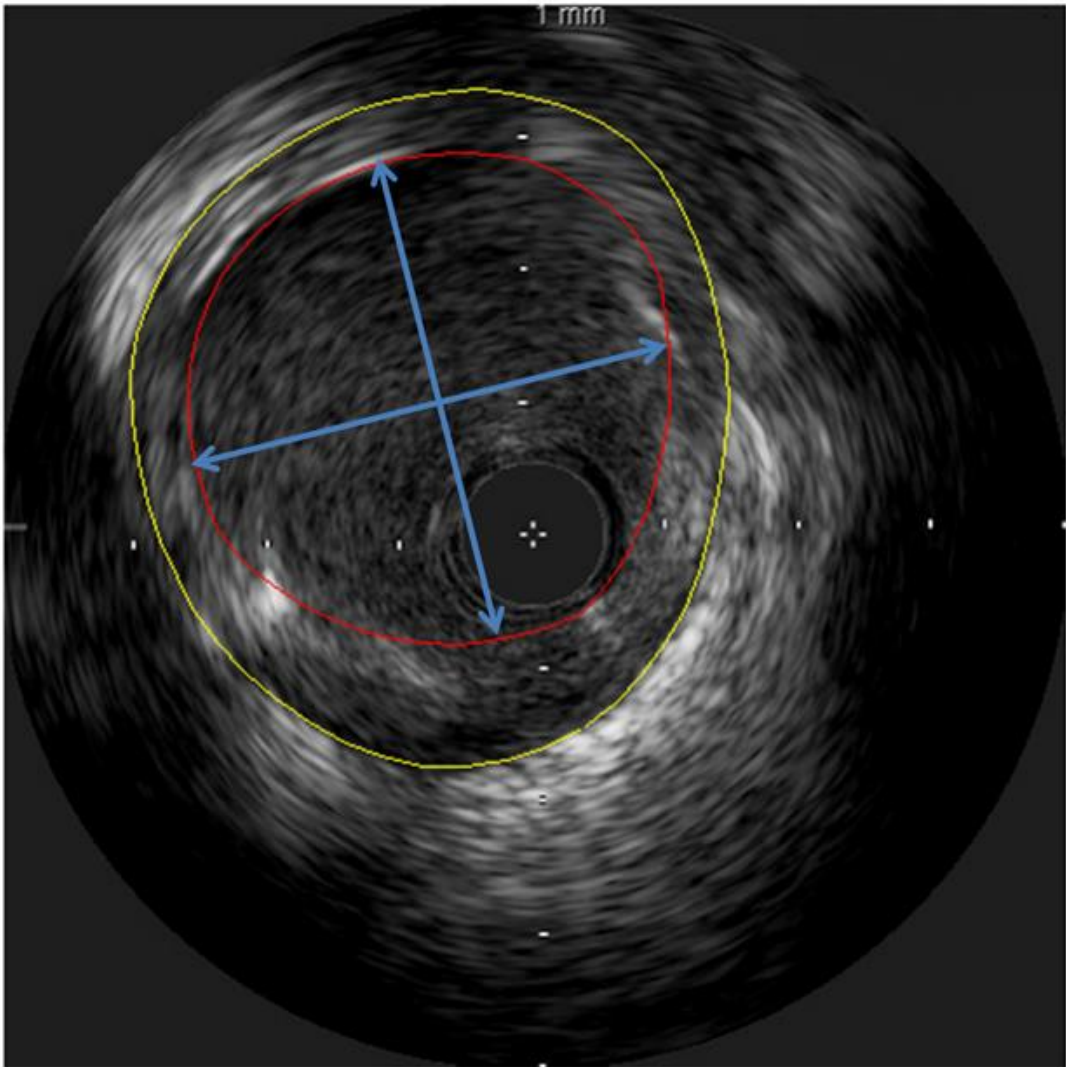


B.

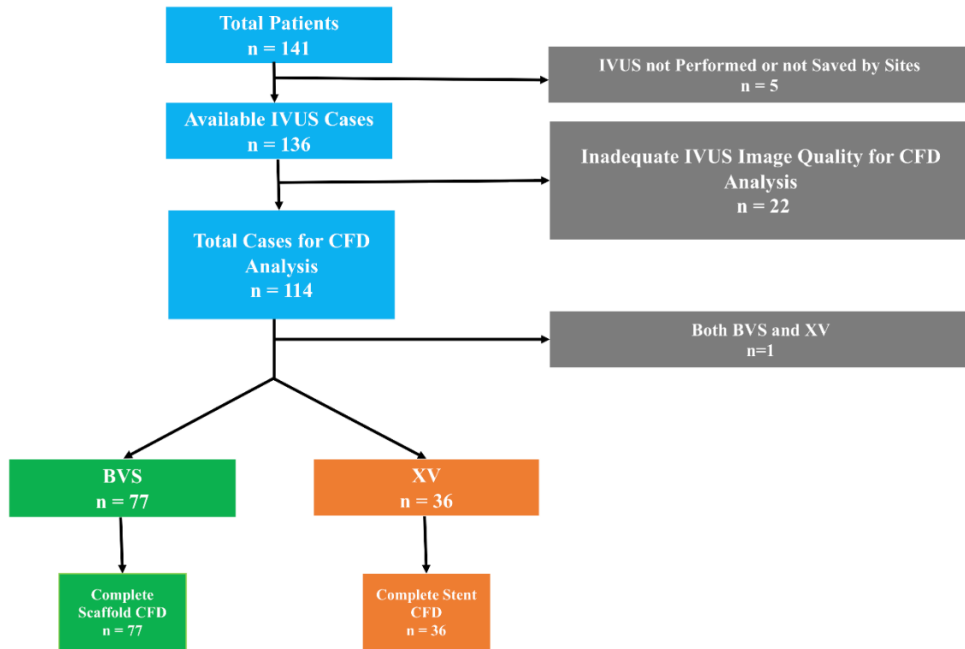


**Supplementary Figure 1.** Derivation of underexpanded frames by the proximal/distal reference method (A) and the tapering reference method (B).

The derived vessel lumen area of the stented region is shown in purple and is used to derive reference lumen areas. The true vessel lumen is shown in transparent brown overlaying the simulated lumen. Red and blue rectangles demonstrate upstream and downstream reference segments that were used to calculate the proximal and distal reference lumen areas (A) and tapering reference lumen areas (B). Frame lumen area ratios  $<0.9$  of their corresponding reference lumen area were defined as underexpanded frames.



**Supplementary Figure 2.** Derivation of eccentricity index.



**Supplementary Figure 3.** Flow diagram of the study cohort.

**Supplementary Table 1. Comparison of baseline demographics, clinical features and lesion characteristics in BVS vs XV groups.**

<b>Patient characteristics</b>	<b>BVS (n=77)</b>	<b>XV (n=36)</b>	<b>p-value</b>
<b>Age, years</b>	64 (54, 73)	65 (57, 72)	0.679
<b>Male</b>	48 (62)	22 (61)	0.901
<b>Body mass index, kg/m<sup>2</sup></b>	29.4 (26.55, 34.35)	30.4 (25.9, 34.5)	0.968
<b>Hypertension</b>	62 (81)	25 (69)	0.192
<b>Hyperlipidaemia</b>	69 (90)	31 (86)	0.587
<b>Diabetes mellitus</b>	30 (39)	14 (39)	0.994
<b>Prior myocardial infarction</b>	17 (22)	7 (19)	0.751
<b>Smoking</b>	43 (56)	21 (58)	0.804
<b>Renal insufficiency (GFR &lt;30 mL/min/1.73 m<sup>2</sup>)</b>	4 (11)	15 (19.5)	0.268
<b>CVA/TIA</b>	3 (4)	3 (4)	0.327
<b>Systolic BP at stent placement, mmHg</b>	140 (122, 155)	139 (128, 153)	0.635
<b>Diastolic BP at stent placement, mmHg</b>	76 (70, 87)	78 (73, 86)	0.403
<b>Target coronary artery location</b>			
<b>Left anterior descending</b>	36 (47)	21 (58)	0.251
<b>Left circumflex artery</b>	21 (27)	8 (22)	0.567
<b>Right coronary artery</b>	20 (26)	7 (19)	0.448
<b>Pre-stent lesion characteristics</b>			
<b>ACC AHA lesion grade &gt;1</b>	72 (95)	36 (100)	0.161
<b>Angiographic lesion length</b>	11.54 (9.33, 15.39)	12.08 (9.86, 14.11)	0.840
<b>Angiographic reference vessel diameter, mm</b>	3 (2.50, 3.50)	3 (3, 3.50)	0.573
<b>Angiographic diameter stenosis, %</b>	68.74 (60.32, 74.50)	67.91 (61.91, 73.56)	0.795
<b>Angiographic minimum luminal diameter, mm</b>	0.81 (0.67, 1.04)	0.80 (0.66, 1.04)	0.995
<b>Post-stent characteristics</b>			
<b>IVUS-derived stent length</b>	19.50 (17.80, 26.80)	19.75 (16.20, 24.55)	0.471
<b>IVUS-derived MLD, mm</b>	2.20 (1.90, 2.40)	2.30 (2.1, 2.6)	0.051
<b>IVUS-derived mean lumen diameter</b>	2.78±0.46	2.81±0.42	0.693
<b>IVUS-derived residual plaque burden, %</b>	54.23 (49.65, 58.64)	52.22 (46.34, 59.05)	0.286
<b>Contrast velocity, mm/sec</b>	139 (120, 169)	148 (114, 177)	0.746

<b>Underexpansion - MUSIC criteria, % frames</b>	31 (7, 79)	35 (0, 96)	0.850
<b>Underexpansion - prox/dist ref. method, % frames</b>	49 (28, 72)	49 (47, 93)	0.106
<b>Underexpansion - tapering ref. method, % frames</b>	54 (22, 86)	73 (44, 97)	0.061
<b>Total stent EI%</b>	10 (6, 13)	7 (5, 9)	0.006

Values are median (interquartile range) or mean±standard deviation.

BP: blood pressure; BVS: Absorb bioresorbable vascular scaffold; CVA: cerebrovascular accident; Dist: distal; GFR: glomerular filtration rate; IVUS: intravascular ultrasound; MLD: minimal luminal diameter; Prox: proximal; ref: reference; TIA: transient ischaemic attack; XV: XIENCE V